



## RESEARCH ARTICLE

# Comprehensive multicentre retrospective analysis for predicting isocitrate dehydrogenase-mutant lower-grade gliomas

Dongxu Zhao<sup>1,†</sup>, Lin Duan<sup>1,†</sup>, Tareq A. Juratli<sup>2,†</sup>, Fazheng Shen<sup>3,†</sup>, Liyun Zhou<sup>1</sup>, Shulin Cui<sup>3</sup>, Hang Zhang<sup>1</sup>, Hang Ren<sup>1</sup>, Luyao Cheng<sup>1</sup>, Hailan Wang<sup>1</sup>, Wenhan Shi<sup>1</sup>, Tianxiao Li<sup>1</sup>  & Ming Li<sup>1</sup> 

<sup>1</sup>Department of Cerebrovascular Disease and Neurosurgery, Henan University People's Hospital, Henan Provincial People's Hospital, Zhengzhou, 450003, China

<sup>2</sup>Department of Neurosurgery, Faculty of Medicine and University Hospital Carl Gustav Carus, Technische Universität Dresden, Dresden, Germany

<sup>3</sup>The First Affiliated Hospital of Xinxiang Medical University, Weihui, 453100, China

## Correspondence

Ming Li and Tianxiao Li, Department of Cerebrovascular Disease and Neurosurgery, Henan University People's Hospital, Henan Provincial People's Hospital, Weiwu Road No.7, Zhengzhou, NC 450003, China. Tel: +86 135 9888 8356; Fax: +86-0371-65580453; E-mail: [mingli@zhu.edu.cn](mailto:mingli@zhu.edu.cn) (M.L.) and Tel: +86 186 0386 9791; Fax: +86-0371-65964376; E-mail: [dr.litianxiao@zhu.edu.cn](mailto:dr.litianxiao@zhu.edu.cn) (T.L.)

Received: 23 August 2024; Revised: 7 October 2024; Accepted: 27 October 2024

doi: 10.1002/acn3.52251

<sup>†</sup>These authors have contributed equally to this work.

## Abstract

**Objective:** To differentiate glioma grading and determine isocitrate dehydrogenase (IDH) mutation status, which are crucial for prognosis assessment and treatment planning in glioma patients. **Methods:** This retrospective study included patients diagnosed with adult diffuse glioma from 1 January, 2018 to 31 July, 2023 in two independent institutions. It documented and analysed clinical and radiographic features. A nomogram model was constructed using stepwise regression to predict lower-grade gliomas and IDH mutation status. **Results:** A total of 383 adult patients with diffuse glioma were included in the study, with Cohort A (297 patients) serving as the training set and Cohort B (86 patients) serving as the validation cohort. Consistent with previous reports, the Hyper fluid-attenuated inversion recovery (FLAIR) rim sign exhibited higher sensitivity in lower-grade gliomas for IDH mutant gliomas compared with the T2-FLAIR mismatch sign. However, the Hyper FLAIR rim sign was also present in Grade 4 gliomas, and thus, the T2-FLAIR mismatch sign exhibited better clinical efficacy in predicting glioma grade and IDH mutation compared with the Hyper FLAIR rim sign in clinical applications. Meanwhile, preoperative magnetic resonance spectroscopy (MRS) indicators, particularly the Cho/Cr ratio, have shown excellent performance in predicting glioma grade and IDH mutation status. The nomogram developed through stepwise regression demonstrated excellent predictive capabilities in distinguishing glioma grade and IDH mutation status. **Interpretation:** Combining imaging and molecular features, the predictive model established in this study offers a reliable non-invasive tool for predicting glioma grading and IDH mutation status, aiding the clinical decision-making process and improving patient management.

## Introduction

Diffuse gliomas are amongst the most common primary tumours of the central nervous system in adults. In 2016, the World Health Organization (WHO) classification of central nervous system tumours incorporated molecular testing results as a key diagnostic criterion for glioma classification for the first time. The 2021 WHO CNS5 classification also highlighted the diagnostic value of

molecular diagnostics in determining glioma subtypes and introduced a distinction between adult-type and paediatric-type gliomas for the first time.<sup>1,2</sup>

With the advancement of molecular testing for gliomas, molecular/genetic characteristics have supplemented standard histological analysis, providing additional diagnostic and prognostic information and even blurring the traditional WHO distinction between low-grade and high-grade gliomas. In recent years, Grades 2 and 3

gliomas are often collectively referred to as 'lower-grade gliomas' (LGGs) to further emphasise their distinction from the more aggressive GBMs.<sup>5</sup> Numerous studies have shown that the IDH gene is a significant factor that affects the prognosis of gliomas. IDH-mutant lower-grade adult diffuse gliomas are more sensitive to radio-chemotherapy and have a longer survival time. Moreover, IDH mutation is a favourable prognostic marker for overall survival improvement in lower-grade gliomas.<sup>4,5</sup>

IDH mutation significantly alters the metabolic activity and breakdown of metabolic products in tumour cells. In cells that exhibit IDH mutation, the conversion of isocitrate to  $\alpha$ -ketoglutarate is inhibited, whilst the production of D-2-hydroxyglutarate (D-2-HG) is increased. D-2-HG is an oncogenic metabolite that plays a major role in the tumorigenesis of gliomas.<sup>6</sup> IDH inhibitors, which can block this pathological function, are amongst the most promising treatments for LGGs. Studies have shown that IDH inhibitors (ivosidenib and vorasidenib) significantly improve the progression-free survival of lower-grade IDH mutant gliomas, underscoring the importance of the non-invasive assessment of IDH mutations for clinical significance.<sup>7,8</sup>

With continuous advancements in neurofunctional imaging techniques and the introduction of new radiographic signs, clinicians can better predict low-grade gliomas and IDH molecular status noninvasively before surgery. Magnetic resonance spectroscopy (MRS), as a method for imaging brain metabolites, plays an important role in assessing glioma grade and IDH status through the Cho/Cr ratio.<sup>9</sup> An elevated Cho/Cr ratio reflects increased cell membrane turnover and metabolic activity, which is typically associated with higher tumour grades and malignancy, making it a useful marker for distinguishing lower-grade gliomas from more aggressive forms like glioblastoma. Additionally, the Cho/Cr ratio correlates with IDH status. IDH mutations may alter tumour cell metabolic pathways, leading to reduced choline metabolism. As a result, lower Cho/Cr values are generally observed in IDH mutant gliomas compared to IDH wild-type tumours.<sup>10</sup> This makes the Cho/Cr ratio valuable in predicting tumour behaviour and guiding preoperative decisions.

This non-invasive prediction of glioma grade and molecular characteristics enables patients to receive more appropriate diagnostic and treatment plans, improving their outcomes. Therefore, the current study established a multifactorial logistic regression model that aimed to predict lower-grade adult diffuse gliomas and IDH status, providing new strategies for developing brain glioma treatment plans, formulating individualised surgical plans and assessing prognosis.

## Methods and Materials

### Patient selection and clinical data

In this study, we meticulously compiled a dataset that comprised 383 adult diffuse glioma cases, which were surgically and pathologically confirmed between January 2018 and July 2023. This dataset was collected from two distinguished institutions: Henan Provincial People's Hospital and the First Affiliated Hospital of Xinxiang Medical University. The patient cohort was structured into two distinct groups: Cohort A, from Henan Provincial People's Hospital, which encompassed 297 cases, and Cohort B, from the First Affiliated Hospital of Xinxiang Medical University, which comprised 86 cases. Our retrospective study was reviewed and approved by the Ethics review Committee of Hospital, No. EC-024-095. All patients participating in the retrospective study provided written informed consent.

The inclusion criteria were stringently defined to ensure the relevance and integrity of the study sample. These criteria included the following: (1) adherence to the established diagnostic standards for adult diffuse gliomas; (2) completion of surgical intervention, followed by the acquisition of postoperative pathological and molecular diagnostic findings for each patient and (3) comprehensive preoperative diagnostic imaging, specifically MRI, MRS and computed tomography (CT) scans, with fully intact data records.

### Collection of radiological data

All patients underwent preoperative MRI, MRS and CT examinations. MRI examinations were performed using the Discovery 3.0T superconducting magnetic resonance 8-channel phased array head coil and the Pioneer 3.0T superconducting magnetic resonance scanner DST Head Neck Unit (General Electric Company, USA). The MRI examination sequences included at least T1-weighted imaging in the axial plane, T2-weighted imaging and fluid-attenuated inversion recovery (FLAIR) sequences. Specific scanning parameters can be found in the Supplementary Materials (Table S1). MRS utilised single-voxel point-resolved spectroscopy technology, with the volume of interest positioned at the tumour edge that measured 15 mm  $\times$  15 mm  $\times$  15 mm. Repetition time was 1500 ms, and echo time was 135 ms. The spectra were generated using internal scanning software, providing automatic peak assignment and ratio calculations.

### Image analysis

The imaging data were independently reviewed by two neuroradiologists with over 10 years of clinical experience

under unknown pathological conditions. In case of differing opinions, a third doctor was consulted for interpretation. The observed MRI morphological features included the following: (1) tumour boundaries, whether distinct or blurred; (2) presence of peritumoural oedema; (3) whether the enhancement sequence exhibited rim enhancement; (4) whether the lesion was primarily located in the frontal lobe; (5) whether the tumour crossed the midline; (6) T2-FLAIR mismatch sign: the tumour presented complete or nearly complete

homogeneous high signal intensity on T2WI and primarily low signal on FLAIR (with possibly uneven suppression), but with a thin high signal margin, T2-FLAIR was typically accompanied by minimal or no enhancement<sup>11</sup> (Fig. 1A) and (7) FLAIR hyperintense rim sign: regardless of T2 sequence characteristics, the presence of a high signal rim on FLAIR alone would suffice<sup>12,13</sup> (Fig. 1B). Qualitative assessment for calcification was performed on CT images. MRS was performed using a single-voxel technique. The voxel was carefully placed at the edge of the

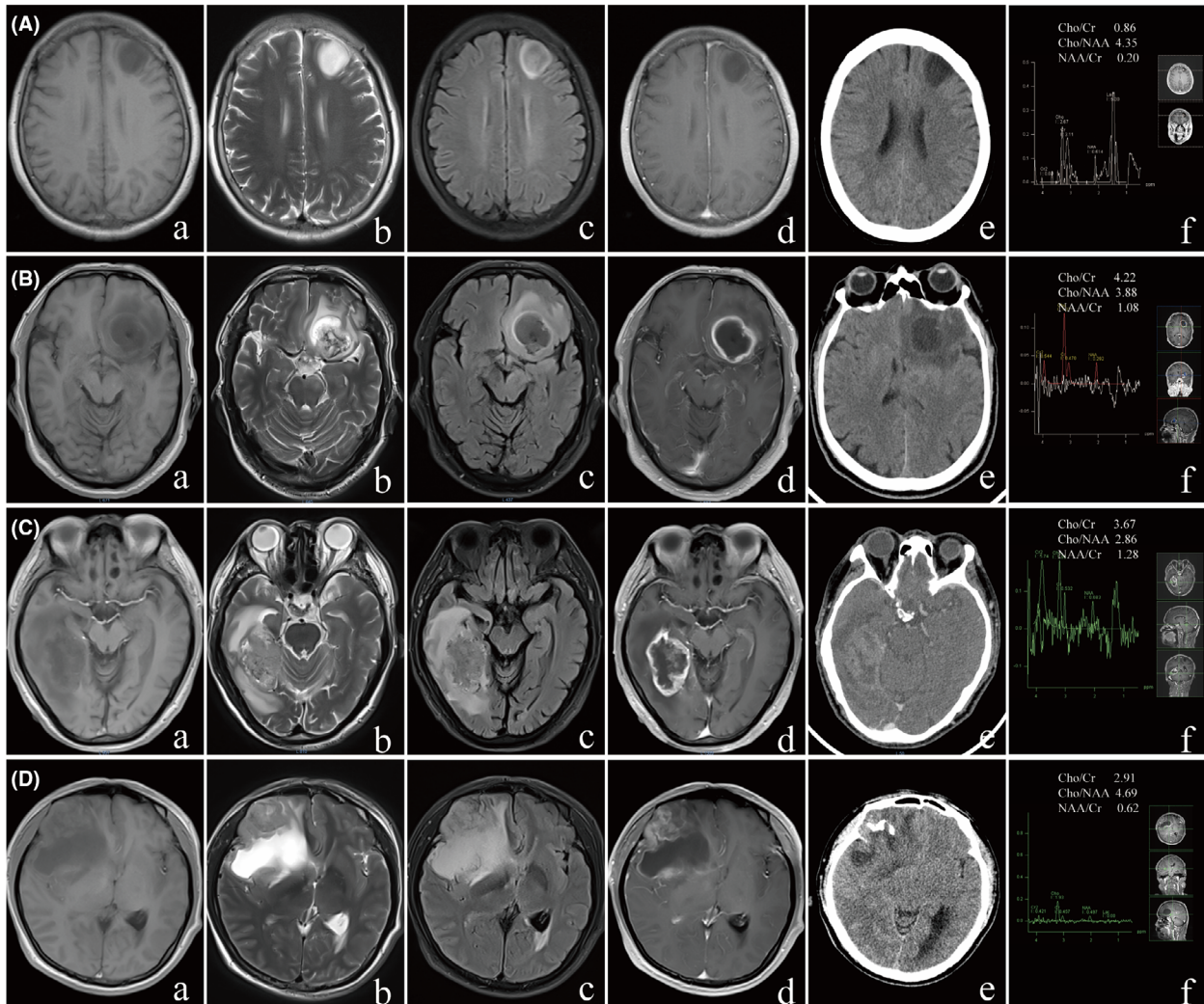


**Figure 1.** Representative examples of IDH mutant and IDH wild-type gliomas: (A) A classic example of a Grade 2 IDHmut non-codeleted glioma with T2-FLAIR mismatch (T2FM). This patient has low signal on T1-weighted imaging (T1WI) (a), uniformly high signal on T2-weighted imaging (T2WI) (b), high signal on the edges with a low signal core on FLAIR (c), smooth margins (b, c), no contrast enhancement (d), no calcification (e) and a low Cho/Cr ratio (f). (B) An IDH wild-type Grade 4 glioblastoma on MRI shows uneven signals (a–d), blurry edges (a, b), extensive peritumoural oedema (c), ring-like enhancement (d), no calcification on CT (e) and uneven T2WI signals with high signal on FLAIR edges and low signal core (b), consistent with the HyperFLAIRrim sign. (C) An IDHwt Grade 4 glioblastoma typically exhibits uneven signals on T2WI with blurry margins (a, b), extensive peritumoural oedema (c), ring-like enhancement (d), no calcification (e) and a high Cho/Cr ratio (f). (D) A patient with a Grade 3 IDHmut-Codel glioma showing low signal on T1WI (a), uneven signal on T2WI (b), no high signal edges and no low signal core on FLAIR (c), partial edge contrast enhancement without forming an enhancement ring (d), calcification on CT (e) and a high Cho/Cr ratio.

glioma, an area chosen for its ability to capture the most metabolically active region of the tumour. Voxel positioning was guided by T2-weighted and FLAIR images to ensure accurate placement and avoid necrotic or cystic areas. MRS scans were acquired using a repetition time (TR) of  $X$  ms and an echo time (TE) of  $Y$  ms, with data automatically processed by the internal software to extract metabolite ratios such as Cho/Cr, NAA/Cr and Cho/NAA.

### Histopathologic and molecular analysis

All tissue specimens were fixed into paraffin blocks and analysed in the Pathology Department of hospital. The tumours were classified into grade 2, 3 and 4, according to 2021 CNS5 classification. In cases where the immunohistochemistry (IHC) test for the IDH1 (R132H) mutant protein was negative, next-generation sequencing (NGS) was used to detect mutations in IDH1 R132 and IDH2 R172. The determination of the IDH genotype was accomplished through a combination of immunohistochemistry and molecular biological testing.

### Statistical analysis

Data analysis was performed using SPSS 25.0, R (version 4.3.2) and R Studio (version 1.2.5033). For the analysis of imaging features and index differences, Shapiro–Wilk tests were first used to assess the homogeneity of variance and normality of the quantitative data (Tables S2 and S3). When data demonstrated homogeneity of variance and approximated a normal distribution, they were presented as mean  $\pm$  standard deviation. Comparisons between two groups were conducted using the independent sample  $t$ -test, and ANOVA was used for multiple group comparisons. For data that did not follow a normal distribution, medians and interquartile ranges (M) were used, and comparisons amongst groups were made using the Mann–Whitney  $U$  test. Qualitative data were analysed using Pearson's chi-squared test or Fisher's exact test for differences between two groups. A significance level of  $\alpha = 0.05$  was set, with  $P < 0.05$  indicating statistical significance.

Independent variables with statistical differences in the test group were selected using stepwise regression in R, and a logistic regression model was then constructed. This model was then adopted to create a nomogram by using data from the test group. The model's performance was evaluated through receiver operating characteristic (ROC) curves, area under the curve (AUC), concordance index and goodness-of-fit tests. Internal validation was conducted using the bootstrap method on the test group data to draw calibration curves. External validation was performed on the validation group to plot ROC curves and

calculate AUC values. The clinical utility of the model was assessed using decision curve analysis.

## Result

### Descriptive characteristics

The investigation encompassed two groups: Cohort A, from Henan Provincial People's Hospital, comprising 297 patients, and Cohort B, from the First Affiliated Hospital of Xinxiang Medical University, with 86 patients (Table 1). Baseline characteristics, including age, gender, tumour grade and IDH mutation status, were compared between the test and validation sets. Statistical analysis showed no significant differences between the two groups in terms of tumour grade ( $P = 0.930$ ), IDH mutation status ( $P = 0.328$ ), age at diagnosis ( $P = 0.408$ ) and gender distribution ( $P = 0.121$ ), indicating that the test and validation sets are comparable.

Individuals with grade 4 gliomas were notably older compared to those with lower-grade gliomas ( $P < 0.001$ ). The separation of lower-grade and grade 4 gliomas was determined through ROC analysis (Fig. S1a), revealing an AUC of 0.761 (95% CI = 0.707 to 0.815), with the optimal diagnostic cut-off offering 62.4% sensitivity and 80.7% specificity, resulting in a Youden index of 0.43. Conversely, those with IDH mutant gliomas were significantly younger than their IDH wild-type counterparts ( $P < 0.001$ ). Discrimination between IDH mutant and wild-type gliomas was assessed via ROC analysis (Fig. S1b), achieving an AUC of 0.761 (95% CI = 0.707 to 0.815), with the diagnostic cut-off demonstrating 60.2% sensitivity, 84.3% specificity and a Youden index of 0.45.

### Imaging characteristics

Regarding MRI morphological characteristics (Tables 2 and 3), previous studies have reported that T2-FLAIR mismatch sign and Hyper FLAIR rim sign in lower-grade gliomas predict IDH mutation with high specificity, nearly 100% and lower sensitivity. This study found that the T2-FLAIR mismatch sign shows statistical significance in distinguishing between lower-grade gliomas and Grade 4 gliomas as well as identifying IDH mutations in both Cohort A and Cohort B (All,  $P < 0.001$ ). The sign was observed in 18 cases (12.9%) of lower-grade gliomas in Cohort A and 7 cases (17%) in Cohort B, with all molecular types being IDHmut non-codeleted astrocytoma (Tables S4 and S5). However, the T2-FLAIR mismatch sign is not present in grade 4 gliomas or in IDHwt gliomas. The Hyper FLAIR rim sign showed statistical significance in distinguishing between lower-grade gliomas and Grade 4 gliomas in Cohort A

**Table 1.** Baseline characteristics of test and validation sets, including molecular subtype of gliomas, patient age at diagnosis and gender.

Characteristics	Test set (n = 297)		Validation set (n = 86)		P
	Grade 2 or 3 (n = 140)	Grade 4 (n = 157)	Grade 2 or 3 (n = 41)	Grade 4 (n = 45)	
Molecular subtype					0.328
IDHmut	110 (78.5%)	11 (7.0%)	28 (68.3%)	2 (4.4%)	
IDHwt	30 (21.5%)	146 (93.0%)	13 (31.7%)	43 (95.6%)	
Age at diagnosis (years)					0.408
Median	48	59	50	58	
Range	20–70	27–83	29–74	20–78	
Gender					0.121
Female	55 (39.3%)	69 (43.9%)	21 (51.2%)	23 (51.1%)	
Male	85 (60.7%)	88 (56.1%)	20 (48.8%)	22 (48.9%)	

P: A comparison between test set versus validation set.

**Table 2.** Comparison of clinical and radiological features of LGGs and HGGs in cohort A and cohort B.

Characteristics	Test set (n = 297)		P	Validation set (n = 86)		P
	Grade 2 or 3 (n = 140)	Grade 4 (n = 157)		Grade 2 or 3 (n = 41)	Grade 4 (n = 45)	
Age	46.2 ± 11.7	58.0 ± 12.0	<0.001	48.2 ± 12.5	58.6 ± 11.1	<0.001
Gender (male/female)	85/55	88/69	0.416	20/21	22/23	0.992
Tumour location			0.005			<0.001
Frontal	59 (42.1%)	42 (26.8%)		28 (68.3%)	13 (28.9%)	
Nonfrontal	81 (57.9%)	115 (73.2%)		13 (31.7%)	32 (71.1%)	
Largest tumour diameter	5.1 ± 1.6	4.7 ± 1.6	0.040	4.6 ± 1.6	5.1 ± 1.4	0.131
Peritumoral oedema	38 (27.1%)	128 (81.5%)	<0.001	11 (26.8%)	43 (95.6%)	<0.001
Tumour boundary			<0.001			<0.001
Clear	86 (61.4%)	32 (20.4%)		22 (53.7%)	2 (4.4%)	
Blur	54 (38.6%)	125 (79.6%)		19 (46.3%)	43 (95.6%)	
Rim enhancement	26 (18.6%)	118 (75.2%)	<0.001	4 (9.8%)	42 (93.3%)	<0.001
Crossing midline	29 (20.7%)	69 (43.9%)	<0.001	3 (7.3%)	21 (46.7%)	<0.001
Calcification	31 (22.1%)	16 (10.2%)	0.005	9 (22.0%)	3 (6.7%)	0.041
T2FM	18 (12.9%)	0 (0%)	0.002	7 (17.1%)	0 (0%)	0.004
Hyper FLAIR rim	23 (16.4%)	7 (4.5%)	<0.001	10 (24.4%)	4 (8.9%)	0.052
Cho/NAA	3.31 (1.96–6.07)	5.60 (3.34–9.10)	<0.001	2.59 (1.69–6.83)	5.12 (2.49–9.26)	0.010
Cho/Cr	1.93 (1.47–2.62)	3.09 (2.18–4.47)	<0.001	1.86 (1.36–2.49)	3.31 (2.08–4.53)	<0.001
NAA/Cr	0.62 (0.40–1.01)	0.59 (0.38–0.97)	0.512	0.65 (0.39–1.23)	0.66 (0.36–1.32)	0.707

P: A comparison between WHO grade 2 or 3 versus WHO grade 4.

( $P < 0.001$ ) but not in Cohort B ( $P = 0.052$ ); it showed statistical significance in identifying IDH mutations in both Cohort A and Cohort B ( $P < 0.001$ ,  $P = 0.005$ , respectively), where it appeared in 23 cases (16.4%) and 10 cases (24.4%) of lower-grade gliomas in Cohort A and Cohort B, respectively, and in 7 cases (4.5%) and 4 cases (8.9%) of Grade 4 gliomas, respectively (example in Fig. 1D); it appeared in 26 cases (19.8%) and 10 cases (30%) of IDH-mut gliomas in Cohort A and Cohort B, respectively, while in IDHwt gliomas, it appeared in 4 cases (2.3%) and 4 cases (7.1%), respectively.

In Cohort A, calcification in the CT scan was observed in 31 cases (22.1%) of lower-grade gliomas compared to 16 cases (10.1%) of Grade 4 gliomas, showing statistical

significance, similar to the findings in Cohort B ( $P = 0.005$ ,  $P = 0.041$ , respectively). When comparing IDHmut gliomas to IDHwt gliomas, in Cohort A, calcification occurred in 28 cases (23.1%) of IDHmut gliomas and 19 cases (10.8%) of IDHwt gliomas (example in Fig. 1C,D), with both showing statistical significance, akin to the results in Cohort B ( $P = 0.004$ ,  $P = 0.03$ , respectively).

### Diagnostic value of MRS

In Cohort A, the differences in Cho/NAA and Cho/Cr ratios between lower-grade gliomas and Grade 4 gliomas were statistically significant ( $P < 0.001$ , All), whereas the NAA/Cr ratio showed no statistical significance between the two

**Table 3.** Comparison of clinical and radiological features between IDH-mutant and IDH wild-type gliomas in cohort A and cohort B.

Characteristics	Test set ( <i>n</i> = 297)		<i>P</i>	Validation set ( <i>n</i> = 86)		<i>P</i>
	IDHmut ( <i>n</i> = 121)	IDHwt ( <i>n</i> = 176)		IDHmut ( <i>n</i> = 30)	IDHwt ( <i>n</i> = 56)	
Age	45.7 ± 10.7	57.1 ± 12.9	<0.001	46.9 ± 10.9	57.3 ± 12.3	<0.001
Gender (male/female)	69/52	104/72	0.723	14/16	28/28	0.768
Tumour location			<0.001			<0.001
Frontal	63 (52.1%)	38 (21.6%)		25 (83.3%)	16 (28.6%)	
Nonfrontal	58 (47.9%)	138 (78.4%)		5 (16.7%)	40 (71.4%)	
Largest tumour diameter	5.4 ± 1.5	4.5 ± 1.5	<0.001	5.4 ± 1.4	4.6 ± 1.6	0.026
Peritumoral edema	40 (33.1%)	126 (71.6%)	<0.001	7 (23.3%)	47 (83.9%)	<0.001
Tumour boundary			<0.001			<0.001
Clear	68 (56.2%)	50 (28.4%)		17 (56.7%)	7 (12.5%)	
Blur	53 (43.8%)	126 (71.6%)		13 (43.3%)	49 (87.5%)	
Rim enhancement	30 (24.8%)	114 (64.8%)	<0.001	3 (10.0%)	43 (76.8%)	<0.001
Crossing midline	29 (24.0%)	69 (39.2%)	0.006	4 (13.3%)	20 (35.7%)	0.027
Calcification	28 (23.1%)	19 (10.8%)	0.004	8 (26.7%)	4 (7.1%)	0.03
T2FM	18 (14.9%)	0 (0%)	<0.001	7 (23.3%)	0 (0%)	<0.001
Hyper FLAIR rim	26 (21.5%)	4 (2.3%)	<0.001	10 (33.3%)	4 (7.1%)	0.005
Cho/NAA	4.10 (2.54–7.36)	4.86 (2.55–8.28)	0.579	5.93 (2.16–8.65)	3.64 (1.79–8.04)	0.143
Cho/Cr	2.20 (1.62–3.22)	2.77 (1.84–4.08)	<0.001	1.97 (1.40–3.59)	2.86 (1.63–3.89)	0.017
NAA/Cr	0.58 (0.37–0.88)	0.62 (0.39–1.08)	0.058	0.57 (0.29–0.94)	0.83 (0.45–1.39)	0.299

*P*: A comparison between IDH mut versus IDH wild-type.

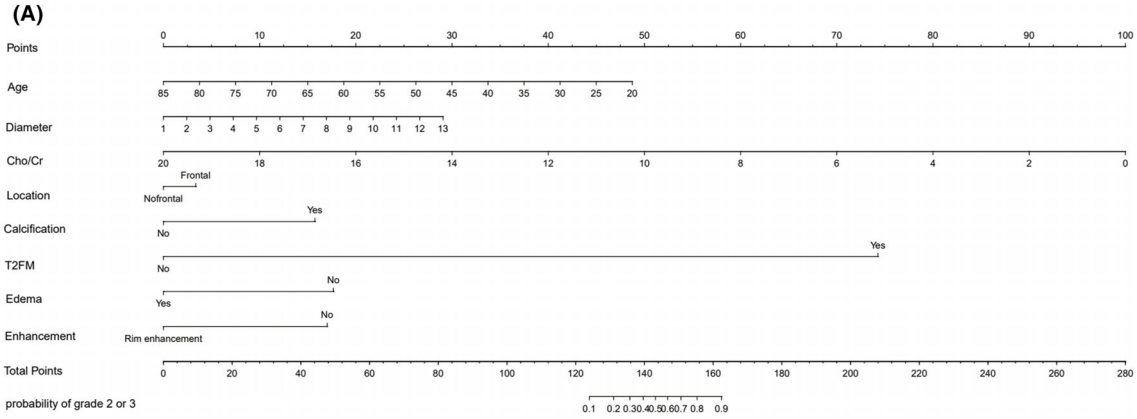
groups; the difference in Cho/Cr ratio between IDH mutant gliomas and IDH wild-type gliomas in Cohort A was statistically significant ( $P < 0.001$ ), while there was no statistical significance in Cho/NAA and NAA/Cr ratios between the two groups. The ROC curve for the Cho/Cr ratio in distinguishing lower-grade gliomas from Grade 4 gliomas (Fig. S2a) had an AUC of 0.737 (95% CI = 0.680–0.793), with an optimal diagnostic cut-off value, a sensitivity of 66.9%, a specificity of 73.6% and a Youden index of 0.405; the ROC curve for the Cho/Cr ratio in distinguishing IDH mutant gliomas from IDH wild-type gliomas (Fig. S2b) had an AUC of 0.611 (95% CI = 0.546–0.675), with an optimal diagnostic cut-off value, a sensitivity of 66.9%, a specificity of 58.0% and a Youden index of 0.249. Therefore, the Cho/Cr ratio can serve as a reliable imaging biomarker, providing quantitative information for the grading and typing of gliomas.

### Nomogram for predicting LGGs

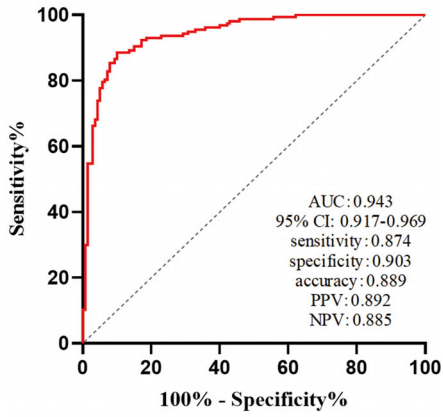
This study incorporated all indices with statistical differences in differentiating glioma grades in the test group into a Logistic regression model. Through stepwise

regression for variable selection, the results indicated that in distinguishing lower-grade gliomas from Grade 4 gliomas, the model constructed from age, maximum tumour diameter, Cho/Cr ratio, whether the tumour is located in the frontal lobe, calcification, T2-FLAIR mismatch sign, peritumoral oedema and rim enhancement (Fig. 2A) exhibited excellent predictive capability for lower-grade gliomas in Cohort A (AUC 0.943, 95% CI 0.917–0.969, Fig. 2B). The detailed Logistic regression results are provided in Table S6. The same model was applied to Cohort B, demonstrating the best predictive ability in Cohort B as well (AUC 0.946, 95% CI 0.903–0.990, Fig. 2C). The nomogram demonstrated good accuracy in assessing the likelihood of lower-grade gliomas (concordance index (C-index) was 0.792). Furthermore, calibration plots showed a good agreement between the actual lower-grade gliomas and the likelihood estimated by the nomogram (Cohort A Fig. 2D, Cohort B Fig. 2E). In addition, decision curve analysis (DCA) was performed to assess the clinical utility of the nomogram. As shown in the DCA curve (Cohort A Fig. 2F, Cohort B Fig. 2G), the nomogram provides a positive net benefit across a wide range of threshold probabilities, particularly between 20% and 60%. This

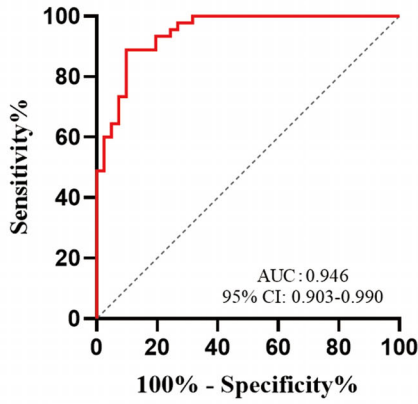
**Figure 2.** Lower-grade Glioma prediction model and model evaluation (A) The nomogram evaluates the scores for predicting lower-grade gliomas through each feature selected by stepwise regression. (B and C) ROC curves of combined predictors for distinguishing lower-grade gliomas from Grade 4 gliomas. The maximal AUC for Cohort A was 0.943 (95% CI 0.917–0.969) and the maximal AUC for Cohort B was 0.946 (95% CI 0.903–0.990). (D and E) The nomogram demonstrates the diagnostic performance effectiveness in predicting lower-grade gliomas in Cohorts A (D) and B (E). (F and G) DCA assesses the clinical utility of the constructed model. The x-axis and y-axis represent the threshold probability and net benefit, respectively.



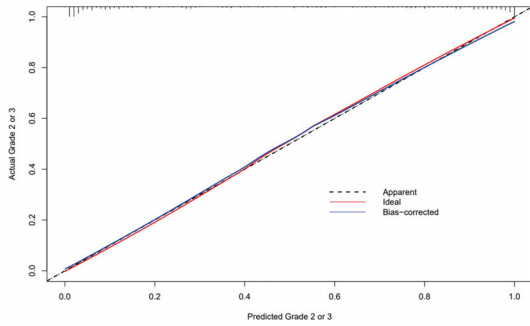
**(B)** ROC Curve for Cohort A



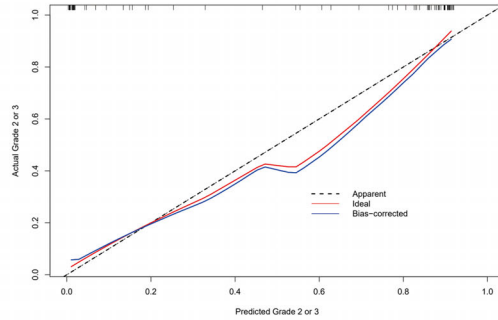
**(C)** ROC Curve for Cohort B



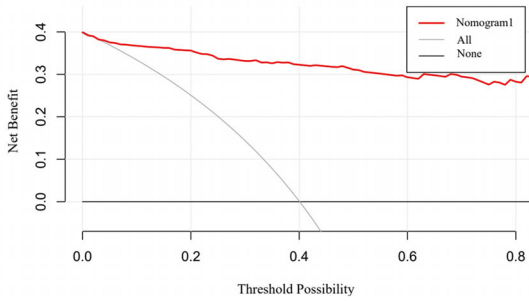
**(D)** Calibration Curve for Cohort A



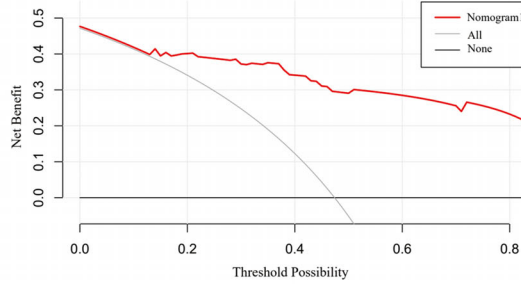
**(E)** Calibration Curve for Cohort B



**(F)** Cohort A



**(G)** Cohort B



indicates that the nomogram can effectively assist clinicians in making informed decisions regarding the diagnosis and treatment of lower-grade gliomas, offering meaningful clinical benefit by identifying patients most likely to benefit from further intervention.

### Nomogram for predicting IDH mutation status

This study included all indicators showing statistical differences in distinguishing IDH mutant from non-mutant gliomas in the test group into a Logistic regression model, and through stepwise regression for independent variable selection, it was found that the model constructed from age, maximum tumour diameter, tumour location in the frontal lobe, calcification, T2-FLAIR mismatch sign, Cho/Cr ratio and enhancement ring (Fig. 3A) had excellent predictive power for IDH mutant gliomas in Cohort A (AUC 0.901, 95% CI 0.864–0.937, Fig. 3B). The detailed Logistic regression results are provided in Table S7. The same model was applied to Cohort B, demonstrating the best predictive ability in Cohort B as well (AUC 0.944, 95% CI 0.888–0.989, Fig. 3C). The nomogram showed good accuracy in assessing the likelihood of IDHmut gliomas (concordance index (C-index) was 0.382). Furthermore, calibration plots demonstrated a good agreement between the actual IDHmut gliomas and the likelihood estimated by the nomogram (Cohort A Fig. 3D, Cohort B Fig. 3E). DCA assessed the clinical utility of this predictive model, indicating that the model is effective in clinical application (Cohort A Fig. 3F, Cohort B Fig. 3G).

### Discussion

As a type of brain tumour with different histological grades and molecular diversity, the tumour grading and molecular type of glioma significantly affect the prognosis and treatment strategies of patients.<sup>1,2</sup> As a molecular biomarker, IDH has been identified in recent years as an ideal target for the precise targeted treatment of IDH mutant gliomas.<sup>14</sup> IDH inhibitors and vaccines have emerged as new treatment modalities for IDH mutant gliomas. IDH inhibitors are a class of small molecule drugs designed to directly target and inhibit the activity of the mutant IDH enzyme, blocking the production of

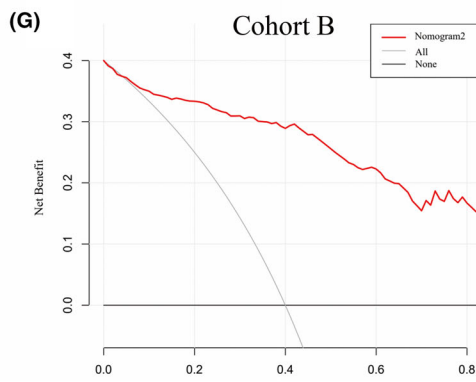
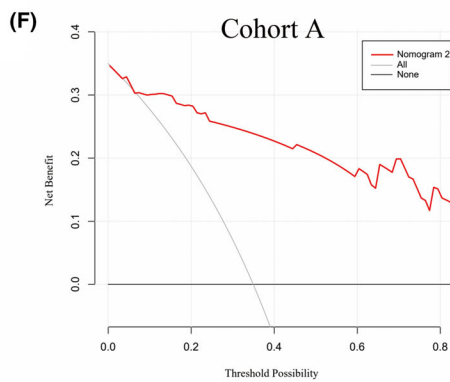
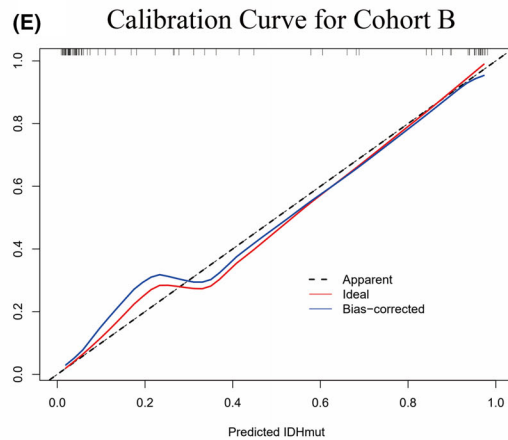
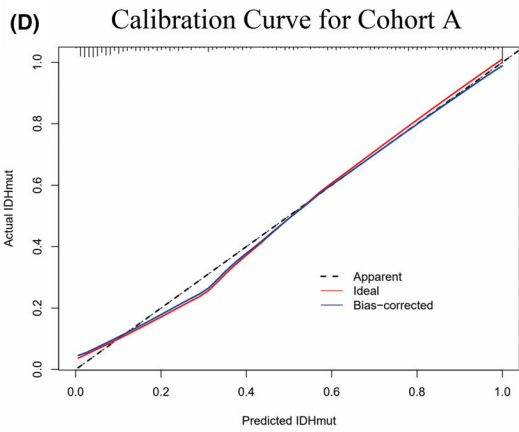
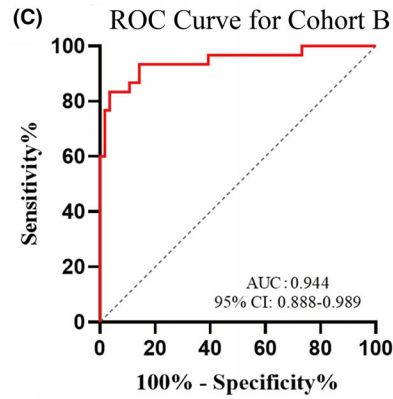
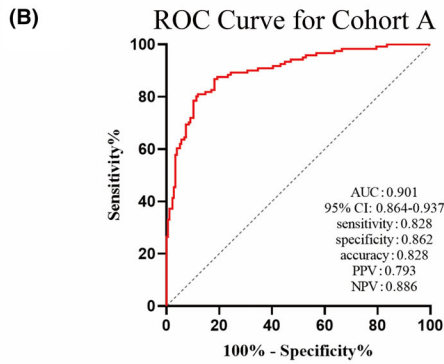
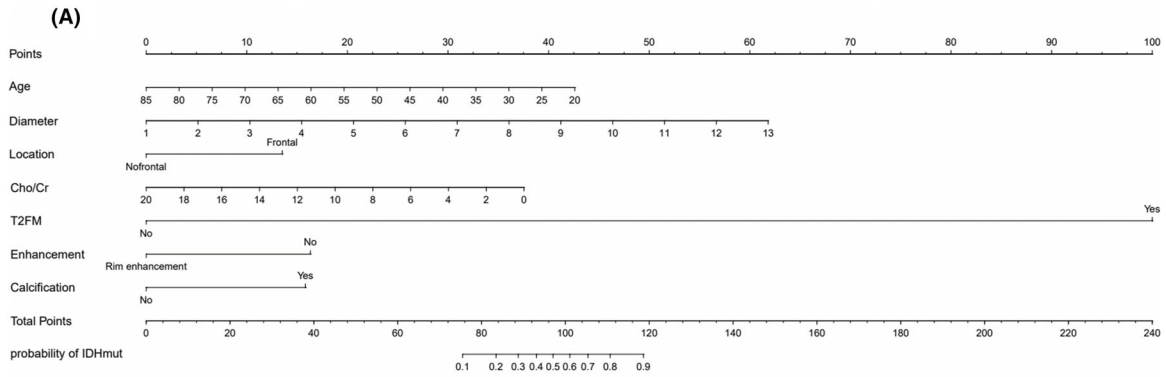
tumour-promoting metabolites and slowing or preventing the proliferation and survival of tumour cells. Previous studies have confirmed that IDH inhibitors, such as ivosidenib and vorasidenib, have extended the progression-free survival of patients with lower-grade IDH mutant gliomas.<sup>7,8</sup> The IDH vaccine, which is an immunotherapy strategy, aims to activate the body's immune system to fight against tumour cells that carry IDH mutation.<sup>15–17</sup>

This study not only conducted statistical analysis on T2-FLAIR mismatch and Hyper FLAIR rim signs in lower-grade gliomas but also compared their application value in Grade 4 gliomas. The T2-FLAIR mismatch sign, which was used to diagnose astrocytomas, exhibited lower sensitivity and extremely high specificity. This finding is consistent with that of the previous research by Patel *et al.*<sup>11,18–23</sup> Notably, the T2-FLAIR mismatch sign appeared in Cohorts A and B in cases molecularly characterised as IDHmut non-codeleted astrocytomas, whilst it was absent in Grade IV and IDHwt gliomas. Johnson *et al.*<sup>24</sup> reported 12 cases of false positives of T2-FLAIR mismatch sign, all occurring in IDHmut-Codel lower-grade oligodendrogliomas. To date, the sign has not been observed in IDHwt lower-grade gliomas. The Hyper FLAIR rim sign, which was firstly proposed by Throckmorton and Graber<sup>12</sup> in 2020, should not rely on T2 sequence features and the FLAIR high signal ring alone is a radiological feature of high sensitivity and specificity for astrocytomas. Subsequently, Li and Lin *et al.*,<sup>13</sup> through the validation of 585 cases of lower-grade gliomas, demonstrated the higher sensitivity and specificity of Hyper FLAIR rim compared with T2-FLAIR mismatch sign in lower-grade gliomas. Although the Hyper FLAIR rim sign exhibited higher sensitivity for IDH mutant gliomas in lower-grade gliomas than the T2-FLAIR mismatch sign, the current study found the presence of Hyper FLAIR rim sign in Grade 4 gliomas, and thus, the T2-FLAIR mismatch sign presented better clinical efficacy in predicting glioma grades and IDH mutations compared with the Hyper FLAIR rim sign in clinical applications.

MRS plays an irreplaceable role in the diagnosis of gliomas by measuring the concentration ratios of different metabolites in the brain, providing important information about gliomas and their biological characteristics. The Cho/Cr ratio is an important indicator, offering key information about tumour cell metabolic activity and malignancy

**Figure 3.** IDHmut Glioma prediction model and model evaluation. (A) The nomogram evaluates the scores for predicting IDHmut gliomas through each feature selected by stepwise regression; (B) and (C) ROC curves of combined predictors for distinguishing IDH mutants from IDH wild-type gliomas. The maximal AUC for Cohort A was 0.901 (95% CI 0.864–0.937) and the maximal AUC for Cohort B was 0.944 (95% CI 0.888–0.989); (D) and (E) The nomogram demonstrates the diagnostic performance effectiveness in predicting IDHmut gliomas in Cohorts A (D) and B (E). (F) and (G) DCA assesses the clinical utility of the constructed model. The x-axis and y-axis represent the threshold probability and net benefit, respectively.





degree. Furthermore, the Cho/Cr ratio has been demonstrated to help differentiate true progression from pseudoprogression in glioblastoma patients, where an elevated Cho/Cr ratio is often associated with true tumour progression, while lower ratios may indicate pseudoprogression.<sup>25</sup> The current study found that in Grade 4 gliomas, the Cho/Cr ratio was significantly higher than in lower-grade gliomas and this ratio could predict IDH status. Nonetheless, compared with the high sensitivity and specificity demonstrated by Changho Choi et al.<sup>26–29</sup> through the MRS detection of 2-HG for identifying IDH mutant gliomas, the Cho/Cr ratio fell slightly short in terms of sensitivity and specificity. Although the MRS detection of 2-HG is considered a more specific method for identifying IDH mutant gliomas, its equipment requirements and technical conditions limit its widespread clinical application. Therefore, the Cho/Cr ratio can serve as a reliable quantitative information provider for the clinical prediction of glioma grading and molecular typing.

Calcification is considered a typical feature of oligodendrogliomas, and tumours of this type, which carry 1p/19q co-deletion and IDH mutation, typically indicate a more favourable prognosis and better response to chemotherapy and radiotherapy. In the current study, calcification appeared in 28 cases (40.6%) and 7 cases (58.3%) of IDHmut-Codel oligodendrogliomas in Cohorts A and B, respectively. This finding is consistent with the meta-analysis results on lower-grade gliomas by Lent et al.<sup>30,31</sup> As the preferred technology for identifying calcifications, the importance of CT in clinical practice should not be replaced by MRI, particularly in glioma typing and treatment planning. Therefore, calcification can serve as an important radiological marker for predicting lower-grade gliomas and IDH status.

The current study demonstrated the effectiveness of combining MRS indicators and radiological features to predict glioma grading and IDH molecular subtypes. The nomogram established in this study provides significant clinical application value and practicability compared to radiomic machine learning models. Unlike radiomic models, which often require complex image processing and advanced computational tools, our nomogram uses variables that are routinely available and quickly assessed by clinicians in everyday practice. This makes the model easier to implement in both specialised and general healthcare settings, ensuring broader accessibility and utility in clinical decision-making, particularly in environments with limited technological resources. However, this study also has limitations, including its retrospective analysis nature; relatively small case enrolment and subjective assessment of radiological markers without quantifying the extent or degree of mismatch in T2-FLAIR, which aligns more closely with clinical practice.

In conclusion, significant differences exist in MRI morphology and MRS indicators amongst different grades and IDH mutation statuses of gliomas. The logistic regression model constructed by combining age, MRI morphological features and MRS indicators significantly improved the accuracy of predicting glioma histopathological grading and IDH molecular subtypes.

## Author Contributions

Dongxu Zhao: Contributed to the conception, design, acquisition, analysis, interpretation of the data, visualization of the data, and drafting of the work. Lin Duan: Contributed to the acquisition, analysis, interpretation of the data, and drafting of the work. Tareq A. Juratli and Fazheng Shen: Contributed to the acquisition, analysis, and visualization of the data. Liyun Zhou and Shulin Cui: Contributed to the acquisition and analysis of the data. Hang Zhang, Hang Ren, Luyao Cheng, Hailan Wang, Wenhan Shi: Contributed to the acquisition, analysis, and visualization of the data. Tianxiao Li: Contributed to the interpretation of the data, project administration, and drafting of the work. Ming Li: Contributed to the conception, design, interpretation of the data, and drafting of the work.

## Acknowledgments

Not applicable.

## Funding Information

This study was supported by the General Program of the National Natural Science Foundation of China (8217102870).

## Disclosures

The authors have no personal, financial or institutional interest in any of the drugs, materials or devices described in this article.

## Data Availability Statement

The data that support the findings of this study are available from the corresponding author upon reasonable request. Due to ethical considerations, the data are not publicly accessible.

## References

1. Louis DN, Perry A, Reifenberger G, et al. The 2016 World Health Organization classification of tumors of the central nervous system: a summary. *Acta Neuropathol.* 2016;131:803–820. doi:10.1007/s00401-016-1545-1

2. Louis DN, Perry A, Wesseling P, et al. The 2021 WHO classification of tumors of the central nervous system: a summary. *Neuro-Oncology*. 2021;23:1231-1251. doi:10.1093/neuonc/noab106
3. Picca A, Bruno F, Nichelli L, Sanson M, Rudà R. Advances in molecular and imaging biomarkers in lower-grade gliomas. *Expert Rev Neurother*. 2023;23:1217-1231. doi:10.1080/14737175.2023.2285472
4. Deluche E, Bessette B, Durand S, et al. CHI3L1, NTRK2, 1p/19q and IDH status predicts prognosis in glioma. *Cancer*. 2019;11:544. doi:10.3390/cancers11040544
5. Olar A, Wani KM, Alfaro-Munoz KD, et al. IDH mutation status and role of WHO grade and mitotic index in overall survival in grade II–III diffuse gliomas. *Acta Neuropathol*. 2015;129:585-596. doi:10.1007/s00401-015-1398-z
6. Sciortino T, Secoli R, d'Amico E, et al. Raman spectroscopy and machine learning for IDH genotyping of unprocessed glioma biopsies. *Cancer*. 2021;13:4196. doi:10.3390/cancers13164196
7. Mellinghoff IK, Lu M, Wen PY, et al. Vorasidenib and ivosidenib in IDH1-mutant low-grade glioma: a randomized, perioperative phase 1 trial. *Nat Med*. 2023;29:615-622. doi:10.1038/s41591-022-02141-2
8. Mellinghoff IK, van den Bent MJ, Blumenthal DT, et al. Vorasidenib in IDH1- or IDH2-mutant low-grade glioma. *N Engl J Med*. 2023;389:589-601. doi:10.1056/NEJMoa2304194
9. Berger TR, Wen PY, Lang-Orsini M, Chukwueke UN. World Health Organization 2021 classification of central nervous system tumors and implications for therapy for adult-type gliomas. *JAMA Oncol*. 2022;8:1493-1501. doi:10.1001/jamaoncol.2022.2844
10. Yano H, Ikegame Y, Miwa K, et al. Radiological prediction of isocitrate dehydrogenase (IDH) mutational status and pathological verification for lower-grade Astrocytomas. *Cureus*. 2022;14:e27157. doi:10.7759/cureus.27157
11. Patel SH, Poisson LM, Brat DJ, et al. T2-FLAIR mismatch, an imaging biomarker for IDH and 1p/19q status in lower-grade gliomas: a TCGA/TCIA project. *Clin Cancer Res*. 2017;23:6078-6085. doi:10.1158/1078-0432.Ccr-17-0560
12. Throckmorton P, Graber JJ. T2-FLAIR mismatch in isocitrate dehydrogenase mutant astrocytomas. *Neurology*. 2020;95:e1582-e1589. doi:10.1212/wnl.0000000000010324
13. Li M, Ren X, Chen X, et al. Combining hyperintense FLAIR rim and radiological features in identifying IDH mutant 1p/19q non-codeleted lower-grade glioma. *Eur Radiol*. 2022;32:3869-3879. doi:10.1007/s00330-021-08500-w
14. Zakharova G, Efimov V, Raevskiy M, et al. Reclassification of TCGA diffuse glioma profiles linked to transcriptomic, epigenetic, genomic and clinical data, according to the 2021 WHO CNS tumor classification. *Int J Mol Sci*. 2022;24:157. doi:10.3390/ijms24010157
15. Bunse L, Rupp A-K, Poschke I, et al. AMPLIFY-NEOVAC: a randomized, 3-arm multicenter phase I trial to assess safety, tolerability and immunogenicity of IDH1-vac combined with an immune checkpoint inhibitor targeting programmed death-ligand 1 in isocitrate dehydrogenase 1 mutant gliomas. *Neurol Res Pract*. 2022;4:20. doi:10.1186/s42466-022-00184-x
16. Chuntova P, Yamamichi A, Chen T, et al. Inhibition of D-2HG leads to upregulation of a proinflammatory gene signature in a novel HLA-A2/HLA-DR1 transgenic mouse model of IDH1R132H-expressing glioma. *J Immunother Cancer*. 2022;10:e004644. doi:10.1136/jitc-2022-004644
17. Platten M, Bunse L, Wick A, et al. A vaccine targeting mutant IDH1 in newly diagnosed glioma. *Nature*. 2021;592:463-468. doi:10.1038/s41586-021-03363-z
18. Broen MPG, Smits M, Wijnenga MMJ, et al. The T2-FLAIR mismatch sign as an imaging marker for non-enhancing IDH-mutant, 1p/19q-intact lower-grade glioma: a validation study. *Neuro-Oncology*. 2018;20:1393-1399. doi:10.1093/neuonc/noy048
19. Corell A, Ferreyra Vega S, Hoefling N, et al. The clinical significance of the T2-FLAIR mismatch sign in grade II and III gliomas: a population-based study. *BMC Cancer*. 2020;20:450. doi:10.1186/s12885-020-06951-w
20. Deguchi S, Oishi T, Mitsuya K, et al. Clinicopathological analysis of T2-FLAIR mismatch sign in lower-grade gliomas. *Sci Rep*. 2020;10:10113. doi:10.1038/s41598-020-67244-7
21. Juratli TA, Tummala SS, Riedl A, et al. Radiographic assessment of contrast enhancement and T2/FLAIR mismatch sign in lower grade gliomas: correlation with molecular groups. *J Neuro-Oncol*. 2018;141:327-335. doi:10.1007/s11060-018-03034-6
22. Kickingereider P, Bendszus M, Wick W, et al. T2/FLAIR-mismatch sign for noninvasive detection of IDH-mutant 1p/19q non-codeleted gliomas: validity and pathophysiology. *Neuroncol Adv*. 2020;2:vdaa004. doi:10.1093/naojnl/vdaa004
23. Lee MK, Park JE, Jo Y, Park SY, Kim SJ, Kim HS. Advanced imaging parameters improve the prediction of diffuse lower-grade gliomas subtype, IDH mutant with no 1p19q codeletion: added value to the T2/FLAIR mismatch sign. *Eur Radiol*. 2019;30:844-854. doi:10.1007/s00330-019-06395-2
24. Johnson DR, Kaufmann TJ, Patel SH, Chi AS, Snuderl M, Jain R. There is an exception to every rule—T2-FLAIR mismatch sign in gliomas. *Neuroradiology*. 2018;61:225-227. doi:10.1007/s00234-018-2148-4
25. Sidibe I, Tensaouti F, Gilhodes J, et al. Pseudoprogression in GBM versus true progression in patients with glioblastoma: a multiapproach analysis. *Radiother Oncol*. 2023;181:109486. doi:10.1016/j.radonc.2023.109486
26. Choi C, Raisanen JM, Ganji SK, et al. Prospective longitudinal analysis of 2-hydroxyglutarate magnetic

- resonance spectroscopy identifies broad clinical utility for the management of patients with IDH-mutant glioma. *J Clin Oncol*. 2016;34:4030-4039. doi:[10.1200/jco.2016.67.1222](https://doi.org/10.1200/jco.2016.67.1222)
27. Molloy AR, Najac C, Viswanath P, et al. MR-detectable metabolic biomarkers of response to mutant IDH inhibition in low-grade glioma. *Theranostics*. 2020;10:8757-8770. doi:[10.7150/thno.47317](https://doi.org/10.7150/thno.47317)
28. Nguyen D, Nguyen D, Le T, et al. Diagnostic algorithm for glioma grading using dynamic susceptibility contrast-enhanced magnetic resonance perfusion and proton magnetic resonance spectroscopy. *Biomed Rep*. 2024;20:56. doi:[10.3892/br.2024.1741](https://doi.org/10.3892/br.2024.1741)
29. Tietze A, Choi C, Mickey B, et al. Noninvasive assessment of isocitrate dehydrogenase mutation status in cerebral gliomas by magnetic resonance spectroscopy in a clinical setting. *J Neurosurg*. 2018;128:391-398. doi:[10.3171/2016.10.Jns161793](https://doi.org/10.3171/2016.10.Jns161793)
30. Robe PAJT, Snijders TJ, van Baarsen KM, et al. Radiological differences between subtypes of WHO 2016 grade II–III gliomas: a systematic review and meta-analysis. *Neuroncol Adv*. 2020;2:vdaa044. doi:[10.1093/noajnl/vdaa044](https://doi.org/10.1093/noajnl/vdaa044)
31. Saito T, Muragaki Y, Maruyama T, et al. Calcification on CT is a simple and valuable preoperative indicator of 1p/19q loss of heterozygosity in supratentorial brain tumors that are suspected grade II and III gliomas. *Brain Tumor Pathol*. 2016;33:175-182. doi:[10.1007/s10014-016-0249-5](https://doi.org/10.1007/s10014-016-0249-5)

## Supporting Information

Additional supporting information may be found online in the Supporting Information section at the end of the article.

**Figure S1.**

**Figure S2.**

**Table S1.**

**Table S2.**

**Table S3.**

**Table S4.**

**Table S5.**

**Table S6.**

**Table S7.**